Effect of different viscoelastic models on free vibrations of thick cylindrical shells through FSDT under various boundary conditions

Hossein Daemi[a] and Hamidreza Eipakchi*

Faculty of Mechanical and Mechatronics Engineering, Shahrood University of Technology, Shahrood, Iran

Abstract.   This paper investigates the free vibrations of cylindrical shells made of time-dependent materials for different viscoelastic models under various boundary conditions. During the extraction of equations, the displacement field is estimated through the first-order shear deformation theory taking into account the transverse normal strain effect. The constitutive equations follow Hooke's Law, and the kinematic relations are linear. The assumption of axisymmetric is included in the problem. The governing equations of thick viscoelastic cylindrical shell are determined for Maxwell, Kelvin-Voigt and the first and second types of Zener's models based on Hamilton's principle. The motion equations involve four coupled partial differential equations and an analytical method based on the elementary theory of differential equations is used for its solution. Relying on the results, the natural frequencies and mode shapes of viscoelastic shells are identified. Conducting a parametric study, we examine the effects of geometric and mechanical properties and boundary conditions, as well as the effect of transverse normal strain on natural frequencies. The results in this paper are compared against the results obtained from the finite elements analysis. The results suggest that solutions achieved from the two methods are ideally consistent in a special range.

Keywords: thick cylindrical shell; viscoelastic models; frequency analysis; first-order shear deformation theory; analytical solution; boundary conditions

1. Introduction

In the field of structural mechanics, a "shell" refers to a curved and three-dimensional element, which is thin in one direction. Although shells are thin and light, they can tolerate out-of-plane loads owing to their curvature. Numerous researchers and scholars have continuously been investigating the behavior of thin-walled and thick-walled cylindrical shells under different loadings. Given the desirable proportion between weight and mechanical strength of the structure, cylindrical shells are one of the most widely used engineering structures. This feature has been utilized in many engineering fields such as mechanics. Vibrational and dynamic behavior of cylindrical shells constitutes one of the most widely applied engineering fields. The most important step in the examination of dynamic behavior in cylindrical shells is to find natural frequencies and mode shapes. That is because the entire dynamic behaviors of a structure are explored on the basis of these two properties. Therefore, it is crucial to thoroughly investigate natural frequencies and mode shapes in order to carry out an optimal design. Conducting various experiments, researchers have found that the theory of thin-walled shells used for a thick-walled cylinder can give rise to fault in determining the natural frequencies. In other

words, the classical theory of thin-walled shells cannot help achieve sufficient accuracy to solve the thick-walled shells problems. That is because this theory underestimates the deflection and overestimates the natural frequency. A thick-walled shell is distinct from a thin-walled shell. One difference is the transverse shear deformation effect, which cannot be discarded in thick-walled shells.

Due to the difficulty of using the three-dimensional theory of elasticity, the approximated theories are used by researchers for analysis of the shells. The first-order shear deformation theory (FSDT) is one of them, which has been adopted by many researchers to cover the effect of shear deformation on thick shells. In the shear deformation theory employed in this paper, the displacement field in the thickness direction is approximated by a linear function of thickness (z) (Mirsky, and Hermann 1958). Suzuki. *et al.* 1981 analyzed the axisymmetric vibrations of a cylinder with variable thickness in the axial direction under clamped and simple boundary conditions. In their paper, they used the classical shell theory (CST) and the theory of improved thick shells. They solved the vibrational equations by applying the power series method. Soedel (1982) generalized the CST by including the effects of rotary inertia and shear deformation. He used the method of separation of variables to solve the equations of motion, to achieve natural frequencies. Bhimaraddi (1984) proposed a higher-order theory to obtain the natural frequencies of circular cylindrical shells. Trigonometric functions were employed to generate separable solutions with unknown coefficients. Suzuki and Leissa (1986) obtained the natural frequency and mode shape of variable-thickness cylindrical shells. The motion equations contained three differential

---

∗Corresponding author, Associate Professor
 E-mail: hamidre_2000@yahoo.com
[a] Ph.D. Student
 E-mail: h_daemi_me@yahoo.com

equations with variable coefficients. They demonstrated that the mode shapes of thickness-variable cylindrical shells were similar to that of constant-thickness cylindrical shells, but their natural frequencies were different. They developed a solution based on sine functions with respect to time and power series with respect to spatial coordinate. Wong and Bush (1993) used the asymptotic expansion to examine the vibrations of cylindrical shells. In this method, the longitudinal, circumferential and radial displacements, as well as the shell frequency, were expanded based on the thickness-to-radius ratio. Buchanan and Yii (2002) studied the effects of homogeneous boundary conditions on vibrations of thick-walled cylindrical shells using the finite elements (FE) method. Pellicano (2007) assumed the longitudinal, peripheral and radial displacement functions for a cylindrical shell with simple and clamped boundary conditions combined with the harmonic functions and Chebyshev polynomials. He compared the results against the experimental and numerical results. El-Kaabazi and Kennedy (2012) examined the natural frequencies and mode shapes of a thin cylinder with variable thickness using Donnell, Timoshenko and Flugge's theory for the clamped, simple and free supports. They calculated the undamped natural frequencies using a numerical algorithm. Using the Rayleigh method, Lee and Kwak (2015) analyzed the vibrations of circular cylindrical shells, while comparing different shell theories. They indicated that Donnell's theory was not accurate enough to calculate natural frequencies. Moreover, there was no difference between the other theories examined in that study. Cammalleri and Costanza (2016) presented a closed-form solution to determine the natural frequencies of a thin cylinder with clamped-end supports. The governing equations were extracted using the modified Love's theory together with Donnell's assumptions and finally analyzed through a semi-analytic method. Zhao *et al*. (2018) proposed a closed-form solution to analyze an anisotropic cylinder taking into account the general boundary conditions based on Donnell's theory. Zhang *et al*. (2018) examined the vibrations of a relatively thick cylindrical shell under general boundary conditions with the improved Fourier cosine series.

The viscoelastic materials are characterized by properties falling between elastic solid and viscous fluid. The mechanical behavior of these materials simultaneously indicates the rigidity level of an elastic body and the effects of friction loss associated with the viscous fluid. Such behavior results in the time-dependent mechanical properties. The viscoelastic materials have been increasingly used in various engineering due to their unique physical and mechanical properties. A great interest has been created in engineers to study and use viscoelastic materials because of their damping behavior. Cox (1968) investigated the wave propagation in a thick, viscoelastic tube containing a Newtonian fluid. He considered the constant thickness and non-uniform moving load in his formulation. The equations were extracted through the theory of elasticity and then were solved analytically. Hamidzadeh and Sawaya (1995) achieved the equations governing the free vibrations of thick composite cylinders made of viscoelastic layers. They adopted the three-

dimensional wave propagation theory and then provided a solution by numerical methods. Zhang *et al*. (2010) carried out a quasi-static analysis of thick cylinders with a constant viscoelastic thickness under the impact uniform internal pressure and axial load, separately. The governing equations were derived based on the three-dimensional elasticity theory and then were solved by separation variables method. Mohammadi and Sedaghati (2012) applied the FE method for vibrations of a multilayer silicon shell with a viscoelastic core for thin and thick cores. They investigated the transient vibrations for both linear and nonlinear models. It was observed that the nonlinear model has more strong damping than the linear one. Eratl *et al*. (2014) examined the effect of rotary inertia on the dynamical behavior of linear viscoelastic cylindrical and conical helicoidal rods using the FE method. Yang *et al*. (2015) explored the damping and free vibrations of thick multilayer cylindrical shells with viscoelastic core under different boundary conditions. Layer-wised and sandwich hypotheses were adopted to describe composite layers and viscoelastic material. They used a new term for displacement field, where the middle layer was expanded as a combination of standard Fourier series and auxiliary functions. In addition, they obtained natural frequencies and loss coefficients through a parametric study. Then, they obtained the characteristic equation of the system using the modified Ritz method. Poloei *et al*. (2017) studied the nonlinear vibrations of a microbeam with a viscoelastic coating by considering the Euler-Bernoulli beam theory under electrostatic excitation. They used the linear mode shape for discretization. Khadem *et al*. (2017) used the perturbation method for vibrations analysis of viscoelastic annular plate through the FSDT. Barati (2017) presented a dynamic model for nanoplates on the viscoelastic foundation. He considered the porosity, hygrothermal loading, and size-dependent effects and solved the governing equations with the Galerkin method. Jithin *et al*. (2018) examined the mechanical properties of a thick-walled hollow viscoelastic cylinder under multi-axial stress conditions. Mokhtari *et al*. (2018) conducted a dynamic analysis of isotropic multilayer cylindrical shells with a fractional viscoelastic core. They adopted Donnell-Mushtari's theory to obtain the structural equations in the outer layer. In modeling the properties of viscoelastic material, this paper used the Zener model owing to its better consistency with experimental results. The governing equation was solved using the Rayleigh-Ritz method. Barretta *et al*. (2018) used a size-dependent elasticity theory to investigate the free vibrations of Timoshenko FG elastic nano-beams. The FG properties were in the thickness direction with a power law formula. So the motion equations were two coupled PDE with constant coefficients. They presented an analytical solution for these equations with different boundary conditions. Similar work has been performed by Apuzzo *et al*. (2018) for an elastic Euler-Bernoulli nano-beam and Barretta *et al*. (2018) for longitudinal vibrations of a rod.

The survey in the literature shows that most papers concerning the dynamic analysis of cylindrical shells used the CST theory for an analytical solution or numerical
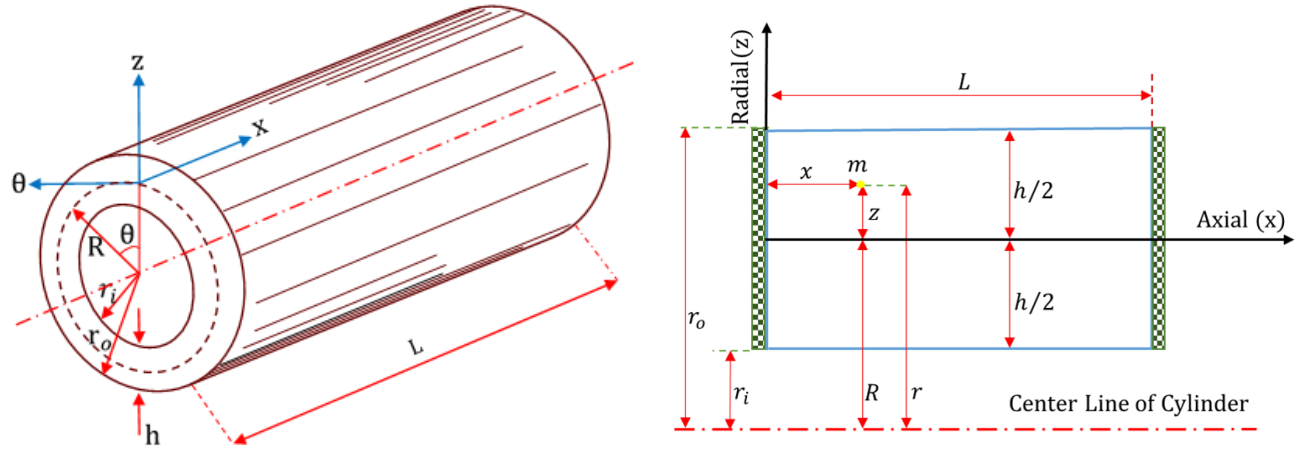
Fig. 1 A cylindrical shell, its longitudinal section and coordinate system (three dimensional and longitudinal section)

methods to the three-dimensional theory of elasticity. Also for viscoelastic properties, the Kelvin model taking into account. In this paper, the governing equations are extracted through the FSDT for the elastic thick-walled cylinders. Then, the equations are extended into the viscoelastic cylindrical equations by the operator method. Finally, the frequency analysis is conducted by solving four coupled partial differential equations. Accordingly, the innovations of this research contain the achievement an analytical procedure for investigating the free vibrations of thick-walled viscoelastic cylinder for different viscoelastic models; investigating the effect of clamped and simply supported boundary conditions on the frequency and mode shapes of viscoelastic thick-walled cylinder for the first Zener model; exploring the effect of neglecting the transverse normal strain on the frequency of the viscoelastic cylinders and surveying the effect of mechanical and material properties on the frequencies for the Zener's models.

2.Equations of motion

2.1 Physics of the problem

As shown in Fig. 1, we consider a cylindrical shell with the inner radius r_i, the outer radius r_o. The shell has the length L, the middle radius R and a constant thickness h. The reference plane for deformation has been considered to be the middle plane, on which the orthogonal coordinate system (x,θ,z) has been located. The displacement components of each point on the cross section in the axial direction x, circular direction θ, and the radial direction have been designated as U_x, U_z, and respectively. The boundary conditions are applied at the two edges. There is no external load in the analysis of free vibrations. The geometric parameters have been displayed in Fig. 1.

2.2 Extraction of elastic cylindrical motion equations

In the first stage, we extracted the equations of motion for the elastic cylinder using Hamilton's principle. Then,

these equations were extended into the viscoelastic state. The equations were based on the FSDT. Also for the extracting the equations of motion we assumed that the shell is homogeneous, isotropic with constant thickness; the problem is axisymmetric i.e $\partial/\partial\theta = 0$ with small displacement, and the stress-strain relations are in accordance with Hooke's law. The shell is viscoelastic and the first and second Zener's models, as well as the Kelvin-Voigt and Maxwell models, are adopted for viscoelastic modeling.

According to Fig. 1, the location of each point in the longitudinal cross-section shell (e.g. m) is defined by two parameters of x and r where r represents the distance from the axis and it is equal to:

$$r = R + z, -\frac{h}{2} \leq z \leq \frac{h}{2}, 0 \leq x \leq L, r_o = r_i + h, R = r_i + \frac{h}{2} \quad (1)$$

Where z is the distance from the middle-plane. The displacement field for the axisymmetric cylinder according to the FSDT by considering the transverse normal strain provides as the following:

$$\begin{bmatrix} U_x(z,x,t) \\ U_z(z,x,t) \end{bmatrix} = \begin{bmatrix} u(x,t) \\ w(x,t) \end{bmatrix} + z.\begin{bmatrix} \varphi(x,t) \\ \psi(x,t) \end{bmatrix}, U_\theta(z,x,t) = 0 \quad (2)$$

$u(x,t)$ and $w(x,t)$ represent the displacement of a point on the middle plane ($z=0$) with the length dimension. $\varphi(x,t)$ is the angle of cross-section rotation on the x-z plane, while $\psi(x,t)$ is the transverse normal strain, which is dimensionless. Moreover, t represents the time.

Mathematically, Eqs. (2) can be regarded as the Taylor expansion of $U_x(x,t)$ and $U_z(x,t)$ around $z=0$, where just two terms are included. According to the strain-displacement equations for the small shell deformation, non-zero components of strains in the axisymmetric state are as follows (Boresi *et al.* 2010):

$$\begin{bmatrix} \varepsilon_x \\ \varepsilon_\theta \\ \varepsilon_z \\ \gamma_{xz} \end{bmatrix} = \begin{bmatrix} \dfrac{\partial U_x}{\partial x} \\ \dfrac{U_z}{r} \\ \dfrac{\partial U_z}{\partial z} \\ \dfrac{\partial U_x}{\partial z} + \dfrac{\partial U_z}{\partial x} \end{bmatrix} = \begin{bmatrix} \dfrac{\partial u}{\partial x} \\ \dfrac{w}{R+z} \\ \psi \\ \varphi + \dfrac{\partial w}{\partial x} \end{bmatrix} + z\begin{bmatrix} \dfrac{\partial \varphi}{\partial x} \\ \dfrac{\psi}{R+z} \\ 0 \\ \dfrac{\partial \psi}{\partial x} \end{bmatrix} \quad (3)$$

Assuming that the behavior of materials is linear, the constitutive equations based on Hooke's law for homogeneous and isotropic materials are as follows (Boresi *et al.* 2010):

$$\sigma_i = I_2\left(\varepsilon_i + \varepsilon_j + \varepsilon_k\right) + \left(I_1 - I_2\right)\varepsilon_i, \ i = x, z, \theta, \ i \neq j \neq k$$
$$\tau_{ij} = \left(I_1 - I_2\right)\gamma_{ij}/2, \quad I_1 = K + 4G/3, \quad I_2 = K - 2G/3 \quad (4)$$

Where K, G are the bulk and the shear modulus. The stress resultants are defined as follows:

$$(N_i, M_i, Q_i) = \int_{-h/2}^{h/2} (1, z, z^2) \cdot \sigma_i \cdot \Omega\, dz, \ i = x, z, \theta;$$

$$\Omega = \begin{cases} 1 + z/R & for \quad i = x, z, xz \\ 1 & for \quad i = \theta \end{cases} \quad (5)$$

$$(N_{xz}, M_{xz}) = K_s \int_{-h/2}^{h/2} (1, z) \cdot \tau_{xz}\left(1 + z/R\right) dz$$

The term $(1+z/R)$ in the stress resultants is not neglected because the cylinder is thick-walled. K_s is the shear correction factor. It is assumed that $K_s = 5/6$ (Vlachoutsis 1992). More detail about the shear correction factor has been reported in the Appendix.

By replacing Eqs. (3), (4) into Eqs. (5), the values of resultants can be obtained in terms of displacement components. The strain energy is calculated as follows:

$$\Pi_U = \pi R \int_0^L \int_{-h/2}^{h/2} (\sigma_x \varepsilon_x + \sigma_\theta \varepsilon_\theta + \sigma_z \varepsilon_z + \tau_{xz}\gamma_{xz})\left(1 + \frac{z}{R}\right) dz\, dx \quad (6a)$$

The kinetic energy is calculated as the following:

$$\Pi_T = \pi R \rho \int_0^L \int_{-h/2}^{h/2} \left(\left[\frac{\partial U_x}{\partial t}\right]^2 + \left[\frac{\partial U_z}{\partial t}\right]^2\right)\left(1 + \frac{z}{R}\right) dz\, dx \quad (6b)$$

Equations of motion are achievable using the Hamilton principle. According to Hamilton's principle in a time interval of (t_1, t_2), we have (Rao 2007).

$$\delta \int_{t_1}^{t_2} (\Pi_T - \Pi_U)\, dt = 0 \quad (6c)$$

δ is the variational operator. By replacing Eqs. (6a), (6b) into Eq. (6c), the governing equations and the boundary conditions can be determined:

$$N_x' = \rho h\left(\ddot{u} + \frac{h^2 \ddot{\varphi}}{12R}\right) \quad (7a)$$

$$M_x' - N_{xz} = \rho\frac{h^3}{12}\left(\ddot{\varphi} + \frac{\ddot{u}}{R}\right) \quad (7b)$$

$$N_{xz}' - \frac{N_\theta}{R} = \rho h\left(\ddot{w} + \frac{h^2 \ddot{\psi}}{12R}\right) \quad (7c)$$

$$M_{xz}' - \frac{M_\theta}{R} - N_z = \frac{\rho h^3}{12}\left(\ddot{\psi} + \frac{\ddot{w}}{R}\right) \quad (7d)$$

$$\left[RN_x\delta u\right]_0^L = 0, \left[RM_x\delta\varphi\right]_0^L = 0, \left[RN_{xz}\delta w\right]_0^L = 0, \left[RM_{xz}\delta\psi\right]_0^L = 0 \quad (7e)$$

The prime and dot specify derivatives relative to *x* and *t*, respectively. Eq. (7e) represents the boundary conditions. The following desired cases are defined for each edge:

- For clamped edge: $u=0$, $w=0$, $\varphi=0$, $\psi=0$.
- For simply supported edge: $u=0$, $w=0$, $M_x=0$, $M_{xz}=0$.
- For free edge: $N_x=0$, $N_{xz}=0$, $M_x=0$, $M_{xz}=0$.

By replacing the resultants Eqs. (5) into Eqs. (7a)- (7d), equations of motion are obtained in terms of displacement components:

$$[A_{11}]\begin{bmatrix} I_1 \\ I_2 \end{bmatrix} + L_1(\ddot{\varphi}, \ddot{u}) = 0 \quad (8a)$$

$$[A_{22}]\begin{bmatrix} I_1 \\ I_2 \end{bmatrix} + L_2\left(\ddot{u}, \frac{h^2}{12}\ddot{\varphi}\right) = 0 \quad (8b)$$

$$[A_{33}]\begin{bmatrix} I_1 \\ I_2 \end{bmatrix} + L_3(\ddot{\psi}, \ddot{w}) = 0 \quad (8c)$$

$$[A_{44}]\begin{bmatrix} I_1 \\ I_2 \end{bmatrix} + L_4\left(\ddot{w}, \frac{h^2}{12}\ddot{\psi}\right) = 0 \quad (8d)$$

Where $L_i, [A_{ii}], i = 1..4$ are as follows:

$$L_i(I_3, I_4) = -\rho h^3 I_3/12 - \rho R h I_4 \quad (8e)$$

$$[A_{11}] = \left[h^3 \varphi''/12 + h R u'' \quad h(R\psi' + w')\right]$$
$$[A_{22}] = \left[h^3 (R\varphi' + u'')/12 - I_5 \quad h^3 \psi'/6 + I_5\right]$$
$$[A_{33}] = \left[\bar{\alpha}\psi - \alpha w + I_6 \quad -h(\psi + u') - I_6\right] \quad (8f)$$
$$[A_{44}] = \left[\bar{\alpha}w - R^2\alpha\psi - I_7 \quad -h(Ru' + w + h^2 \varphi'/6) + I_7\right]$$

$$I_5 = K_s\left(Rh(\varphi + w')/2 + h^3 \psi'/24\right)$$

$$I_6 = I_5', \quad I_7 = -K_s h^3 (\varphi' + w'' + R\psi'')/24 \quad (8g)$$

$$\alpha = \ln\left((2R + h)/(2R - h)\right), \bar{\alpha} = \alpha R - h$$

The equations of motion of thick elastic cylindrical shell include a system of four coupled partial differential equations with constant coefficients. By assuming the material behavior as *viscoelastic in shear* and *elastic in bulk*, the equations are extended for viscoelastic materials.
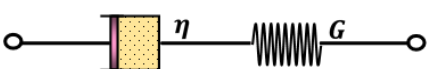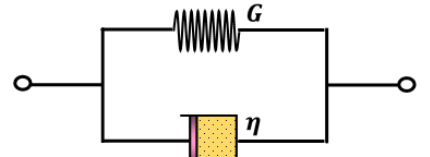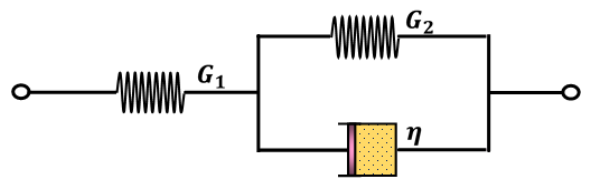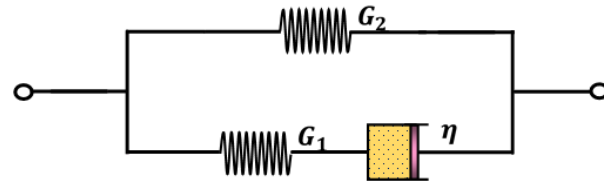
2.3 Extended equations for viscoelastic cylinders

In order to describe the viscoelastic behavior of a system, the *deviatoric* and *dilatational* parts of stress tensor are separated. For the shear part, we have (Skrzypek and Ganczarski 2015):

$$P_1\tau_{ij} = Q_1\varepsilon_{ij} \quad (9)$$

P_1 and Q_1 represent viscoelastic operators τ_{ij} and ε_{ij} represent shear stress and strain. The bulk and shear modulus are determined as follows:

Table 1 Different viscoelastic models

No.	Model	J_4	J_3	J_2	J_1
1	Maxwell	2	0	$1/G$	$1/\eta$
2	Kelvin- Voigt	2η	$2G$	0	1
3	Zener (First type)	$2\eta/G_2$	2	$\eta/G_1 G_2$	$1/G_1 + 1/G_2$
4	Zener (Second type)	$2 + 2G_2/G_1$	$2G_2/\eta$	$1/G_1$	$1/\eta$

$$G = Q_1/2P_1, \quad K = K_0 \tag{10}$$

Where K_0 is the elastic bulk modulus. Since this paper comparatively evaluated four popular viscoelastic models, the following parametric form has been considered for reducing the formulation:

$$P_1 = J_1 + J_2 D, \quad Q_1 = J_3 + J_4 D \tag{11}$$

Where $D = \partial/\partial t$ is the time derivative operator. Moreover, J_1 to J_2 obtain from Table 1 according to selected viscoelastic model. By replacing Eqs. (10), (11) into Eqs. (8a)-(8d) and applying the differential operator, the equations of motion for the viscoelastic thick cylindrical shell is obtained in terms of displacement components.

$$\frac{1}{12}\Lambda_1\left(h^2\phi + 12Ru\right) + \Xi_2\left(w + R\psi\right)' = 0 \tag{12a}$$

$$\frac{h^2}{18}\Lambda_1\left(u + R\phi\right) + \frac{h^2}{36}\Xi_3\psi' - K_s RQ_1\left(w' + \phi\right) = 0 \tag{12b}$$

$$\frac{h}{24}\Lambda_2\left(h^2\psi + 12Rw\right) + \frac{K_s h R}{2}Q_1\phi' - \frac{\alpha_0}{3}\Xi_1 w - \frac{h}{3}\Xi_2 u' + \Xi_4\psi = 0 \tag{12c}$$

$$\frac{h^3}{24}\Lambda_2\left(w + R\psi\right) - \frac{\alpha_0 R^2}{3}\Xi_1\psi - \frac{hR}{3}\Xi_2 u' - \frac{h^3}{72}\Xi_3\phi' + \Xi_4 w = 0 \tag{12d}$$

In these equations, the derivation operators of Ξ_j for $j=1…4$ and Λ_j are defined as follows:

$$\Xi_j = \theta_{j0} + \theta_{j1}D$$

$$\Lambda_1 = \Xi_1\frac{\partial^2}{\partial x^2} - 3\rho P_1\frac{\partial^2}{\partial t^2} \tag{12e}$$

$$\Lambda_2 = K_s Q_1\frac{\partial^2}{\partial x^2} - 2\rho P_1\frac{\partial^2}{\partial t^2}$$

θ_{ji} for $i=0,1$ are expressed in the following forms.

$$\theta_{1i} = 3K_0 J_i + 2J_{i+2}, \quad \theta_{2i} = 3K_0 J_i - J_{i+2}$$

$$\theta_{3i} = 12K_0 J_i - \left(3K_s + 4\right)J_{i+2} \tag{12f}$$

$$\theta_{4i} = K_0\left(\alpha_0 R - 2h\right)J_i + \left(2\alpha_0 R - h\right)J_{i+2}/3$$

3. Analytical solution

The theory of differential equations is essentially based on the determination of system's eigenvalues and eigenvectors. The equations of motion for the viscoelastic thick cylindrical shell, including four third-order (relative to time) and second-order (relative to spatial coordinate) partial differential equations, homogeneous with constant coefficients. The eigenvalues are natural frequencies and eigenvectors are mode shapes of the shell. The equations of motion can be represented as the following form:

Table 2 Characteristics of cylinder

Length (m)	$L=0.775$	Poisson's ratio	$v=0.3$
Middle radius (m)	$R=0.155$	Shear correction factor	$K_s=5/6$
Thickness (m)	$h=R/10$	Density (Kg/m³)	$\rho=7800$
Elasticity modulus (Pa)	$E=2.550e8$	Viscoelastic coefficient (Pa·s)	$\eta=2.744e6$
Bulk modulus (Pa)	$K_0=2.125e8$	Viscoelastic modulus (Pa)	$G_1=9.808e7$, $G_2=2.450e7$

$$\left[\overline{B_8}\right]\frac{\partial y}{\partial x}+\left[\overline{B_7}\right]\frac{\partial^2 y}{\partial x^2}+\left[\overline{B_6}\right]\frac{\partial y}{\partial t}+\left[\overline{B_5}\right]\frac{\partial^2 y}{\partial t^2}+$$
$$\left[\overline{B_4}\right]\frac{\partial^3 y}{\partial t^3}+\left[\overline{B_3}\right]\frac{\partial^2 y}{\partial x\partial t}+\left[\overline{B_2}\right]\frac{\partial^3 y}{\partial x^2\partial t}+\left[\overline{B_1}\right]y=\{0\} \quad (13)$$
$$\{y\}=\{u \quad \varphi \quad w \quad \psi\}^T$$

Where $\{y\}$ includes the dependent functions of equations system. Matrix elements $[\overline{B_1}]$ to $[\overline{B_8}]$ are coefficients of terms in Eqs. (12a)-(12d). For solving the above system of equations, we consider the solution as follows:

$$\{y\}=\{V(x)\}e^{i\omega t} \quad (14)$$

Where ω and $V(x)$ represent the complex frequency and mode shape, respectively. By replacing Eq. (14) into Eqs. (13), the following system of equations is obtained.

$$\left(\left[\overline{B_7}\right]+i\omega\left[\overline{B_2}\right]\right)\frac{\partial^2 V}{\partial x^2}+\left(\left[\overline{B_8}\right]+i\omega\left[\overline{B_3}\right]\right)\frac{\partial V}{\partial x}+\left[\overline{B_0}\right]V=\{0\}$$
$$\left[\overline{B_0}\right]=\left(\left[\overline{B_1}\right]-\omega^2\left[\overline{B_5}\right]\right)+i\left(\omega\left[\overline{B_6}\right]-\omega^3\left[\overline{B_4}\right]\right) \quad (15)$$

The solution of Eq. (15), which is a system of differential equations with constant coefficients, can be considered as follows:

$$\{V(x)\}=\{A\}e^{\beta x} \quad (16)$$

$\{A\}$ is the eigenvector while β is the eigenvalue. By replacing Eq. (16) into Eqs. (15), we have:

$$\left[\beta^2\left(\left[\overline{B_7}\right]+i\omega\left[\overline{B_2}\right]\right)+\beta\left(\left[\overline{B_8}\right]+i\omega\left[\overline{B_3}\right]\right)+\left[\overline{B_0}\right]\right]\{A\}=\{0\} \quad (17)$$

For a non-zero solution, the determinant of coefficients matrix Eq. (17), has to equate to zero, i.e:

$$\det\left(\beta^2\left(\left[\overline{B_7}\right]+i\omega\left[\overline{B_2}\right]\right)+\beta\left(\left[\overline{B_8}\right]+i\omega\left[\overline{B_3}\right]\right)+\left[\overline{B_0}\right]\right)=0 \quad (18)$$

Eq. (18) is the dispersion equation, and its solution specifies eight eigenvalues β_j, $j=1..8$ and eigenvectors. For each eigenvalue, there is an eigenvector determined by Eq. (17). These eigenvalues and eigenvectors include ω. After finding the eigenvalues and eigenvectors, the general form of Eq. (15) is determined as follows:

$$\{V(x)\}=\sum_{j=1}^{8}C_j\{A\}_j\,e^{\beta_j x} \quad (19)$$

Where the constants C_j are determined from the boundary conditions. By applying the boundary conditions

Table 3 Coefficients of Prony's series

Model	q_i	τ	G_0
Maxwell	1	$\dfrac{\eta}{G_1}$	G_1
First Zener's model	$\dfrac{G_1}{G_1+G_2}$	$\dfrac{\eta}{G_1+G_2}$	G_1
Second Zener's model	$\dfrac{G_1}{G_1+G_2}$	$\dfrac{\eta}{G_1}$	G_1+G_2

on two edges of cylindrical shells, an algebraic equations system is derived with eight homogeneous equations that can be formulated in the following matrix form.

$$[ax]\{C\}=\{0\} \quad (20)$$

Where $\{C\}$ includes C_j, $j=1..8$ elements. In order to obtain a non-trivial solution, it is necessary to vanish the determinant of coefficients matrix Eqs. (20).

$$\det[ax]=0 \quad (21)$$

This determinant leads to a complicated algebraic equation in terms of ω that can be solved numerically through the Bisection algorithm. The calculated frequency is a complex number as $\omega=\omega_N+i\alpha_d$, which $\omega_N=\text{Re}(\omega)$ is the natural frequency and $\alpha_d=\text{Im}(\omega)$ is the decay rate of displacement (damping). "Re" and "Im" represent the real and imaginary parts of a complex number, respectively. After determining the values of complex frequency, the mode shapes are determined through Eqs. (15). From eight Eqs. (20), just seven equations are independent. Moreover, C_2-C_8 can be obtained in terms of C_1 from Eqs. (15). The system response is as follows:

$$\{y\}=C_1\{V(x)\}e^{i\omega t}+C.C. \quad (22)$$

Where $C.C.$ represents the complex conjugate of the proceeding terms.

3.1 Effect of transverse normal strain

The statement $\psi(x,t)$ in the equations of motion is the transverse normal strain. By setting $\psi(x,t)=0$ in the equations of motion and removing the fourth equation, we achieve three equations without the effect of normal strain. This has been discussed in the Results section.

4. Numerical solution

Abaqus and Ansys are two popular commercial packages for FE analysis. Ansys does not support the linear

Table 4 Dimensionless natural frequencies- Viscoelastic (S-S)

	First	Second	Third
Elastic (G=G_1)	6.7478	10.4795	10.9480
Elastic (G=G_1) (FE)	6.1611	10.3296	10.9037
Second Zener's model	7.4373	11.6256	12.0695
Second Zener's model (FE)	6.7693	11.5073	12.1841
First Zener's model	6.7524	10.4763	10.9500
First Zener's model (FE)	6.0625	10.2960	10.8890
Maxwell (G_1)	6.7412	10.4464	10.9513
Maxwell (G_1) (FE)	6.0554	10.2935	10.8984
Kelvin-Voigt (G_1)	17.2418	25.1395	27.3565

Table 5 Effect of elasticity modulus G_1 on first frequency of Zener's models (S-S)

Elasticity Modulus(G_1)→	9.81e6	1e7	3.81e7	6.81e7	9.81e7	1e8	3.81e8	9.81e8
First Zener's model	2.1345	2.1549	4.0655	5.6344	6.7464	6.8914	13.6056	21.6143
First Zener's model (FE)	1.9148	1.9372	3.7740	5.0456	6.0554	6.1168	11.9314	19.1487
Second Zener's model	3.5253	3.5431	5.2245	6.4553	7.4373	7.4936	13.7266	21.6756
Second Zener's model (FE)	3.5813	3.5913	4.8376	5.8836	6.7693	6.8224	12.3091	19.3864

Table 6 Effect of elasticity modulus G_2 on first frequency of Zener's models (S-S)

Elasticity Modulus (G_2)→	2.45e2	2.45e3	2.45e4	2.45e5	2.45e6	2.45e7	2.45e8
First Zener's model	6.7895	6.7895	6.7895	6.7895	6.7893	6.7464	6.7697
First Zener's model (FE)	6.0554	6.0554	6.0554	6.0554	6.0554	6.0554	6.0554
Second Zener's model	6.7534	6.7534	6.7540	6.7592	6.8071	7.4373	11.1403
Second Zener's model (FE)	6.0554	6.0554	6.0631	6.0631	6.1303	6.7693	11.3256

Table 7 Effect of thickness-to-radius ratio on frequencies of first Zener's model

h/R→	0.01	0.05	0.1	0.12	0.15	0.2	0.5	0.75	1	1.5	2
First frequency	6.7024	6.7545	6.7524	6.7516	6.7710	6.7749	6.7961	6.8225	6.6696	6.3678	5.7538
First frequency (FE)	6.6873	6.4779	6.1622	6.0324	5.8447	5.5443	4.3126	3.6614	3.2167	2.6432	2.3176
Second frequency	10.3640	10.4285	10.4763	10.4799	10.5284	10.5633	11.0177	11.4259	11.6707	11.9186	11.1631
Second frequency (FE)	10.3832	10.3774	10.3774	10.3000	10.2423	10.1066	9.0858	8.4810	8.1028	7.6556	7.3924

modal analysis for viscoelastic structures. So we employed Abaqus software for numerical analysis. Abaqus uses the Prony series for introducing the viscoelastic material properties. So in order to model the viscoelastic behavior in shear state, the elasticity modulus G has been defined based on the Prony series. The bulk modulus in constant in our study and it has been determined using elastic Young's modulus and Poisson's ratio in the software. Abaqus calculates the bulk modulus through $K_0=E/3(1-2v)$. The shear behavior is as the following:

$$G(t) = G_0\left(1 - \sum_{i=1}^{n} q_i \left(1 - \exp(-t/\tau_i)\right)\right) \qquad (23)$$

G_0 is the instant modulus at t=0. We use just one term of the series, i.e n=1 and the modulus ratio q_i and the relaxation time τ for different mentioned models have been introduced in Table 3. The shear modulus in the Kelvin-Voigt model does not define with a Prony's series.

Also in the FE modeling, the axisymmetric elements with four sides and eight nodes have been used. So it is sufficient to draw just the longitudinal section of the shell in the software environment (Fig. 1). The specifications of the cylinder have been presented in Table 2.

5. Results and discussion

In order to explore the efficiency of the presented formulation, some numerical examples were investigated. We considered a thick-walled cylindrical shell with geometric properties and materials listed in Table 2. All the calculations are based on the data reported in this table except that the mentioned values. The calculations were conducted on the mathematical software Maple 15. In the case studies, the results of natural frequencies were provided for different viscoelastic models. Then, we

Table 8 Natural frequencies with and without transverse normal strain effect (S-S)

Mode number			First	Second
$\bar{h} = 0.1$	First Zener's model	$\psi \neq 0$	6.7524	10.4763
		$\psi = 0$	6.9449	10.6078
		FE	6.0625	10.2960
	Second Zener's model	$\psi \neq 0$	7.4373	11.6256
		$\psi = 0$	7.6286	11.7714
		FE	6.7693	11.5073
$\bar{h} = 0.9$	First Zener's model	$\psi \neq 0$	6.6985	11.6178
		$\psi = 0$	6.8582	11.6039
		FE	3.4526	8.3028
	Second Zener's model	$\psi \neq 0$	7.3131	12.5834
		$\psi = 0$	7.4931	12.7928
		FE	3.3770	8.8710
$\bar{h} = 1.8$	First Zener's model	$\psi \neq 0$	5.91549	11.4378
		$\psi = 0$	6.2119	12.011
		FE	2.4648	7.5139
	Second Zener's model	$\psi \neq 0$	6.5734	12.5928
		$\psi = 0$	6.7603	13.0933
		FE	2.4038	8.1606

surveyed the effects of changing in the geometrical parameters, mechanical properties, supports conditions, and the effect of transverse normal strain on the natural frequencies.

5.1 Frequency analysis

Table 4 provides the values of three natural frequencies obtained from the mathematical analysis of the cylindrical shell with simply supported edges for different viscoelastic models. In order to explain the difference between the viscoelastic and elastic behaviors in thick-walled cylindrical shells, we presented the natural frequency of the elastic shell too. The frequencies were rendered dimensionless through $\bar{\omega} = \omega(R^2/h)\sqrt{\rho/K_0}$. According to Table 4, the frequency of the viscoelastic material is not greater than the elastic case in general and it depends on the type of viscoelastic model, the viscoelastic coefficient, and elasticity modulus. The comparison of the frequency values obtained using different viscoelastic models with the FE analysis shows a good agreement between the results. The difference percentage is an absolute value of $((A_{FE} - A_{AN})/A_{FE})$, where A_{FE} represent the results of the FE and A_{AN} represents the results of the analytical solution. In this paper, the boundary conditions were indicated by two symbols, i.e. the first is at $x=0$ and at is $x=L$. The symbols C, S indicate clamped and simple supports respectively so C-S stands of the clamped at $x=0$ and simply supported at $x=L$ and so on. Furthermore, the dimensionless parameters $\bar{h}$ and $\bar{R}$ have been defined as $\bar{h} = h/R$ and $\bar{R} = R/L$.

Evidently, under identical conditions, the natural frequency in the second model is about 12% higher than that in the first Zener model.

By setting $G_1=\infty$ in the first Zener's model, a Kelvin-Voigt model is obtained. Also for $G_2=0$, it is converted to a Maxwell model. Comparing of the Kelvin-Voigt and Maxwell models shows that the natural frequency in Kelvin-Voigt case is higher than the series state. In Tables 5,6, it has been explained that the variation of G_1 can affect significantly on the frequencies but G_2 has a small variation on the frequency. So the results of the first Zener's model is close to the Maxwell model.

Table 5 reports the natural frequency variations with the modulus of elasticity G_1 for Zener's models, taking into account simply supported edges. As can be seen, an increase in G_1 leads to the greater natural frequency. As the values of G_1 grow, an abrupt increase occurs in natural frequency for a special range. The results are in a good agreement with the FE.

Table 6 represents the natural frequency variations with the modulus of elasticity G_2 for Zener's models. The calculations suggested that as elasticity modulus G_2 varies within $2.45e2 < G_2 < 2.45e8$, there is no significant change in the natural frequency of first Zener's model. In the second Zener's model, however, the frequency is constant within $2.45e2 < G_2 < 2.45e7$. As for $G_2 > 2.45e7$ the natural frequency increases abruptly. Also Tables 5,6 show that the effect of G_1 is more important than G_2 on the frequencies in the studied range.

Table 7 demonstrates the effects of thickness on the frequencies of the viscoelastic cylinders with simple supports. It is seen that, when the cylinder near toward a solid cylinder (rod), the difference between the results increases. Also, this table shows a validity range for the FSDT theory so that the results are valid for $h/R < 0.1$ in this study. Note that increasing the thickness can affect the
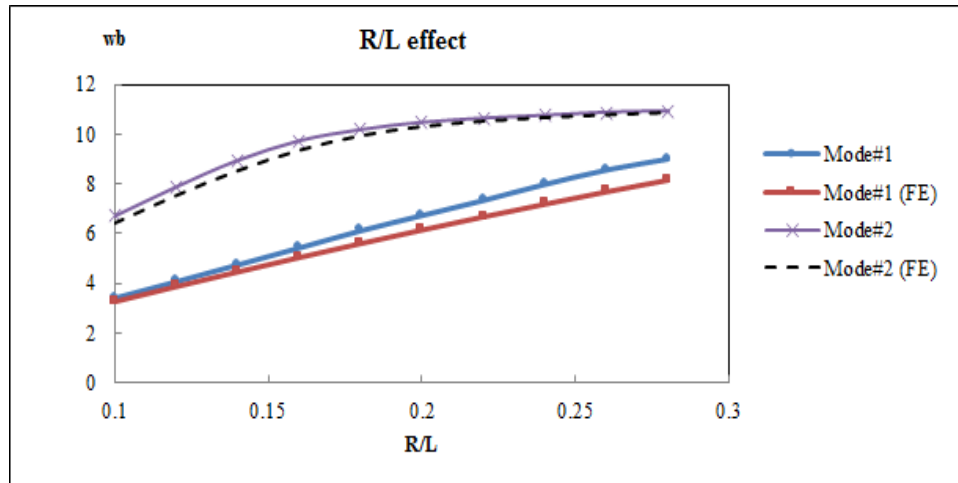
Fig. 2 Effect of radius-to-length ratio on first and second natural frequencies for first Zener's model Mode#1: $\overline{\omega_1} = a_1.\bar{R} + b_1$; Mode#2: $\overline{\omega_2} = b_2.\bar{R}^2 + c_2.\bar{R} + d_2$ FE: a_1=27.330, b_1=0.627; Analytical: a_1=31.470, b_1=0.373 FE: b_2=-185.200, c_2=93.950, d_2=-1.039; Analytic: b_2=-188.600, c_2=93.060, d_2=-0.542
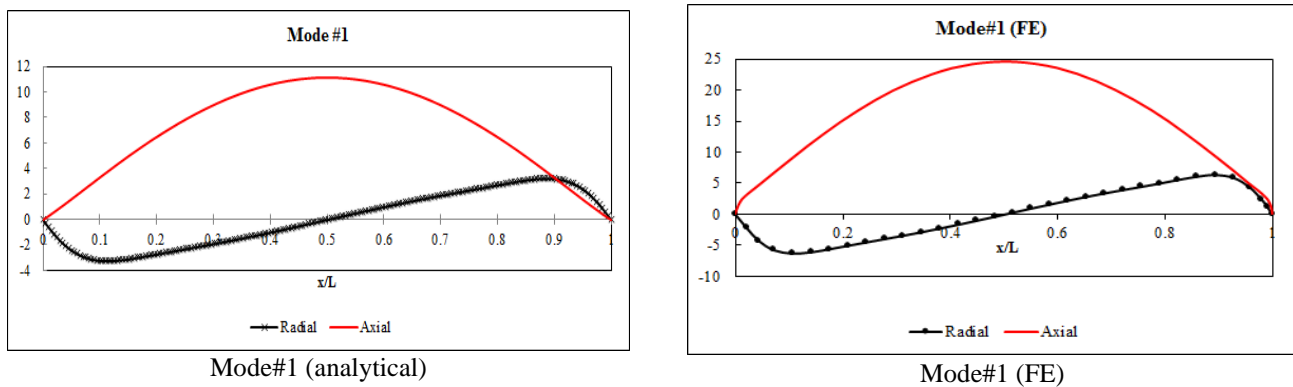

Mode#1 (analytical)

Mode#1 (FE)

Fig. 3 First axial and radial modes for a cylindrical shell with first Zener's model (S-S, analytical and FE)

stiffness and mass of the shell simultaneously thus it is not possible to judge that increasing of the thickness will essentially increase the frequency.

Table 8 expresses the natural frequencies corresponding to the first two modes of motion. When the effect of transverse normal strain is neglected, the results are discrepant by about 5%. It seems that for the specified input data, this effect is more important for thicker shells and higher vibrational modes. In the valid defined range, this parameter does not have a significant effect on the results.

Fig. 2 displays the effect of length variations on the first and second frequencies of the viscoelastic cylinder (first Zener's model) with simply supported edges. The natural frequency chart has been presented in terms of $\bar{R}$. According to the graph, frequency increases as $\bar{R}$ grows i.e. when the cylinder shortens. The frequency variations at greater lengths are negligible in the second natural frequency. Meanwhile, the frequency variations at greater lengths increases in the first frequency. These variations can be approximated by polynomial functions for the frequencies in the studied range. The first and second frequencies variations can be stated as linear and parabolic form respectively.

In Table 9, there are three natural frequencies for the cylindrical shell, considering first Zener's model with

Table 9 Natural frequencies for first Zener's model under different boundary conditions

Mode number	First	Second	Third
C-C	6.8106	10.5794	11.0205
C-C (FE)	6.8013	10.5674	10.9940
C-S	6.7904	10.5228	10.9833
C-S (FE)	6.4567	10.4559	10.9474
S-S	6.7524	10.4763	10.9500
S-S (FE)	6.0625	10.2960	10.8890

Table 10 Effect of viscoelastic coefficient η on first and second frequencies and damping for first Zener's model(S-S)

$n_{i\rightarrow}$		1	2	3	4	5
First mode	$\overline{\omega}$	3.1423	3.1419	3.1508	3.5718	6.7341
	α_d	0	0.0031	0.0315	0.0357	0.0673
Second mode	$\overline{\omega}$	4.7934	4.7955	4.7891	5.1405	9.7624
	α_d	0	0.0096	0.0479	0.0514	0.0976
$n_{i\rightarrow}$		6	7	8	9	10
First mode	$\overline{\omega}$	6.7524	6.7471	6.7477	6.7478	6.7478
	α_d	0.0675	0.0135	0	0	0
Second mode	$\overline{\omega}$	10.4704	10.4816	10.4795	10.4795	10.4795
	α_d	0.0942	0.0210	0	0	0

different boundary conditions. As expected, C-C has the maximum frequency. Also, the agreement between the FE and analytical solutions for the simply supported case is less than the others. In fact, in an analytical solution, the number of mathematical operation is larger than C-C and C-S.

Damping (Imaginary part of complex frequencies) is a criterion for amplitude decay. Table 10 displays the effect of different values of the viscoelastic coefficient on damping.

"n_i" represents the power of viscoelastic coefficient which is defined as $\eta=2.744\exp(n_i.\ln(10))$, $1 < n_i < 10$. $\bar{\omega}$ is dimensionless frequency and α_d is damping (section 3). Table 10 indicates that the damper becomes a rigid connector for large values of n_i. According to this Table, for $\eta > 2.744e7$ and $\eta < 2.744$, there is very small and nearly-zero damping. Also, Table 10 displays the effect of changing the viscoelastic coefficient η on the natural frequency assuming simply supported edges. The results indicated that natural frequency remains nearly constant within $\eta > 2.744e7$ and $\eta < 2.744e3$. Moreover, the frequency decreases for $2.744e3 < \eta < 2.744e7$ as the viscoelastic coefficient decreases for the studied range.

Figs. 3 provide the axial and radial modes for cylindrical shells with first Zener's model and the simply supported boundary conditions. The mode shapes of the FE results have been drawn for comparison too.

6. Conclusions

This paper attempted to analyze the free vibrations of viscoelastic cylindrical shells with constant thickness for different viscoelastic models under various boundary conditions. In this research, the equations governing the system dynamics were obtained by the FSDT with transverse normal strain effect. Then, the equations were extended based on the operator method from elastic to viscoelastic. Finally, the obtained partial differential equations with constant coefficients were solved through the elementary theory of differential equations. By examining the tables and graphs, the following results were obtained for free vibrations of case studies:

• The natural frequency of the viscoelastic thick-walled shell is higher than elastic shells just in certain viscoelastic models.

• By discarding the transverse normal strain from the displacement field equation, a little effect on the natural frequency of the system is shown in the present study.

• Under identical conditions, the natural frequency in the second Zener's model was about 10% higher than the frequency in the first Zener's model.

• For models containing two elements of spring and damper, the frequency of the Kelvin-Voigt model was larger than the frequency of the Maxwell model.

• In the first Zener's model, G_1 has a significant effect on the natural frequencies at the studied range.

• The change in the modulus of elasticity G_2 does not considerably effect the frequency within $2.45e2 < G_2 < 2.45e7$.

• As the viscoelastic coefficient for the first Zener's

models dropped in $2.744e3 < \eta < 2.744e7$, the natural frequency decreases.

• As the thickness increases, the second frequency increases within the interval of $\bar{h} < 0.75$ and decreases within the interval $0.75 < \bar{h} < 2$.

• As the cylinder is shortened, the natural frequency rises. Frequency changes due to increased length at the second natural frequency are associated with a nearly sharp increase.

• The natural frequency was examined in three different boundary conditions. As expected, the maximum and minimum natural frequencies were achieved by C-C and S-S, respectively.

References

Apuzzo, A., Barretta, R., Faghidian, S.A., Luciano, R., and de Sciarra, F. M. (2018), "Free vibrations of elastic beams by modified nonlocal strain gradient theory", *J. Eng. Sci.*, **133**, 99-108. https://doi.org/10.1016/j.ijengsci.2018.09.002.

Barretta, R., Faghidian, S.A., Luciano, R., Medaglia, C.M., and Penna, R. (2018), "Free vibrations of FG elastic Timoshenko nano-beams by strain gradient and stress-driven nonlocal models", *Compos Part B. Eng.*, **154**, 20-32. https://doi.org/10.1016/j.compositesb.2018.07.036.

Barretta, R., Faghidian, S.A., and Luciano, R. (2018), "Longitudinal vibrations of nano-rods by stress-driven integral elasticity", *Mech. Adv. Mater. Struct.*, **26**(15), 1307-1315. https://doi.org/10.1080/15376494.2018.1432806.

Bhimaraddi, A. (1984), "A higher order theory for free vibration analysis of circular cylindrical shells", *J. Solids Struct.*, **20**(7), 623-630. https://doi.org/10.1016/0020-7683(84)90019-2.

Boresi, A.P, Chong, K. and Lee, J.D. (2010), *Elasticity in Engineering Mechanics*, John Wiley and Sons, New Jersey, U.S.A.

Barati, M.R. (2017), "Vibration analysis of FG nanoplates with nanovoids on viscoelastic substrate under hygro-thermo-mechanical loading using nonlocal strain gradient theory", *Struct. Eng. Mech.*, **64**(6), 683-693. https://doi.org/10.12989/sem.2017.64.6.683.

Buchanan, G.R. and Yii, C.B.Y. (2002), "Effect of symmetrical boundary conditions on the vibration of thick hollow cylinders", *Appl. Acoustics*, **63**, 547-566. https://doi.org/10.1016/S0003-682X(01)00048-2.

Cammalleri, M. and Costanza, A. (2016), "A closed-form solution for natural frequencies of thin-walled cylinders with clamped edges", *J. Mech. Sci.*, **110**, 116-126. https://doi.org/10.1016/j.ijmecsci.2016.03.005.

Čanađija, M., Barretta, R., and de Sciarra, F. M. (2016), "On functionally graded Timoshenko nonisothermal nanobeams", *Compos. Struct.*, **135**, 286-296. https://doi.org/10.1016/j.compstruct.2015.09.030.

Cox, R.H. (1968), "Wave propagation through a newtonian fluid contained within a thick-walled, viscoelastic tube", *Biophys. J.*, **8**, 691-709. https://doi.org/10.1016/S0006-3495(68)86515-4.

El-Kaabazi, N. and Kennedy, D. (2012), "Calculation of natural frequencies and vibration modes of variable thickness cylindrical

shells using the Wittrick–Williams algorithm", *Comput. Struct.*, **104**, 4-12. https://doi.org/10.1016/j.compstruc.2012.03.011.

Eratl, N., Argeso, H., Çalım, F.F., Temel, B., Mehmet H. Omurtag, M.H. (2014), "Dynamic analysis of linear viscoelastic cylindrical and conical helicoidal rods using the mixed FEM", *J. Sound Vib.*, **333**, 3671-3690. https://doi.org/10.1016/j.jsv.2014.03.017.

Jithin, A.J., Jung, D.W., Lakshmi, R.R., and Sanal Kumar, V.R. (2018), "Mechanical characterization of a thick-walled viscoelastic hollow cylinder under multiaxial stress conditions", *Mater. Sci. Forum*, **917**, 329-336. https://doi.org/10.4028/www.scientific.net/MSF.917.329.

Hamidzadeh, H.R. and Sawaya, N.N. (1995), "Free vibration of thick multilayer cylinders", *Shock Vib.*, **2**(5), 393-401. https://doi.org/10.3233/SAV-1995-2505.

Khadem Moshir, S., Eipakchi, H.R., and Sohani, F. (2017), "Free vibration behavior of viscoelastic annular plates using first order shear deformation theory", *Struct. Eng. Mech.,,***62**(5), 607-618. https://doi.org/10.12989/sem.2017.62.5.607.

Lee, H. and Kwak, M.K. (2015), "Free vibration analysis of a circular cylindrical shell using the Rayleigh–Ritz method and comparison of different shell theories", *J. Sound Vib.*, **353**, 344-377. https://doi.org/10.1016/j.jsv.2015.05.028.

Mirsky, I. and Hermann, G. (1958), "Axially motions of thick cylindrical shells", *Appl. Mech.*, **25**, 97-102.

Moghtaderi, S.H., Faghidian, S.A., and Shodja, M.H. (2018), "Analytical determination of shear correction factor for Timoshenko beam model", *Steel Compos. Struct.*, **29**(4), 483-491. https://doi.org/10.12989/scs.2018.29.4.483.

Mohammadi, F. and Sedaghati, R. (2012), "Linear and nonlinear vibration analysis of sandwich cylindrical shell with constrained viscoelastic core layer", *J. Mech. Sci.*, **54**(1), 156-171. https://doi.org/10.1016/j.ijmecsci.2011.10.006.

Mokhtari, M., Permoon, M.R. and Haddadpour, H. (2018), "Dynamic analysis of isotropic sandwich cylindrical shell with fractional viscoelastic core using Rayleigh–Ritz method", *Compos. Struct.*, **186**, 165-174. https://doi.org/10.1016/j.compstruct.2017.10.039.

Pellicano, F. (2007), "Vibrations of circular cylindrical shells: theory and experiments", *J. Sound Vib.*, **303**,154-170. https://doi.org/10.1016/j.jsv.2007.01.022.

Poloei, E., Zamanian, M., and Hosseini, S.A.A. (2017) "Nonlinear vibration analysis of an electrostatically excited micro cantilever beam coated by viscoelastic layer with the aim of finding the modified configuration", *Struct. Eng. Mech.,* **61** (2), 193-207. https://doi.org/10.12989/sem.2017.61.2.193.

Rao, S.S. (2007), *Vibration of Continuous Systems*, John Wiley and Sons, U.S.A.

Romano, G., Barretta, A., and Barretta, R. (2012), "On torsion and shear of Saint-Venant beams", *European J. Mech. A/Solids*, **35**, 47-60. https://doi.org/10.1016/j.euromechsol.2012.01.007.

Skrzypek, J.J. and Ganczarski, A.W. (2015), *Mechanics of Anisotropic Materials*, Springer, Heidelberg, Germany.

Soedel, W. (1982), "On the vibration of shells with Timoshenko-Mindlin type shear deflections and rotatory inertia", *J. Sound Vib.,* **83**(1), 67-79. https://doi.org/10.1016/S0022-460X(82)80076-X.

Suzuki, K., Konno, M. and Takahashi, S. (1981), "Axisymmetric vibrations of a cylindrical shell with varying thickness", *Bullet. Japan Soc. Mech. Eng.*, **24**(198), 2112-2132. https://doi.org/10.1299/jsme1958.24.2122.

Suzuki, K. and Leissa, A.W. (1986), "Exact solutions for the free vibrations of open cylindrical shells with circumferentially varying curvature and thickness", *J. Sound Vib.*, **107**(1), 1-15. https://doi.org/10.1016/0022-460X(86)90278-6.

Vlachoutsis, S. (1992), "Shear correction factors for plates and shells", *Numeric. Methods Eng.*, **33**, 1537-1552. https://doi.org/10.1002/nme.1620330712.

Wong, S.K. and Bush, W.B. (1993), "Axisymmetric vibrations of a clamped cylindrical shell using matched asymptotic expansions", *J. Sound Vib.*, **160**(3), 523-531. https://doi.org/10.1006/jsvi.1993.1042.

Yang, C., Jin, G., Liu, Z., Wang, X. and Miao, X. (2015), "Vibration and damping analysis of thick sandwich cylindrical shells with a viscoelastic core under arbitrary boundary conditions", *J. Mech. Sci.*, **92**, 162-177. https://doi.org/10.1016/j.ijmecsci.2014.12.003.

Zhang, W., Fang, Z., Yang, X.D. and Liang, F. (2018), "A series solution for free vibration of moderately thick cylindrical shell with general boundary conditions", *Eng. Struct.*, **165**, 422-440. https://doi.org/10.1016/j.engstruct.2018.03.049.

Zhang, W., Cui, W., Xiao, Z. and Xu, X. (2010), "The quasi-static analysis for the viscoelastic hollow circular cylinder using the symplectic system method", *J. Eng. Sci.*, **48**, 727–741. https://doi.org/10.1016/j.ijengsci.2010.03.003.

Zhao, J., Choe, K., Zhang,Y., Wang, A., Lin, C. and Wang, Q. (2018), "A closed form solution for free vibration of orthotropic circular cylindrical shells with general boundary conditions", *Compos Part B. Eng.*, **159**, 447-460. https://doi.org/10.1016/j.compositesb.2018.09.106.

CC

Appendix

- *Elastic material*

On the basis of the elementary beam theory for a rectangular cross-section the shear stresses τ_{xz} are given according to the quadratic parabola:

$$\tau_{xy} = \frac{3Q_z}{2A}\left(1-(\frac{2z}{h})^2\right) \tag{a1}$$

Because the FSDT formulation uses linear variation in the thickness direction the shear stress distribution in the section is constant which is not compatible with the elasticity theory. So it is usual to apply a correction factor in obtained shear stress to compensate for the constant distribution effect of the stress. Most researchers adopted that this correction factor depends on the aspect ratio and Poisson's ratio. Moghtaderi *et al.* (2018), Čanađija *et al.* (2016) and Romano *et al.* (2012) proposed some analytical relations for the shear correction factor for elastic and FG materials. A typical formula for an elastic rectangular cross-section is as follows (en.wikipedia.org/wiki/Timoshenko_beam_theory):

$$K_s = 10(1+\nu)/(12+11\nu) \tag{a2}$$

- *Viscoelastic material*

In this case, the correction factor is a function of time (*t*). By the procedure mentioned in the paper, we convert Eq. (a2) to the viscoelastic form. For the first Zener's model it results in:

$$(105K_0 + 2G_1)\tau\frac{dK_s(t)}{dt} + (105G_0^* + 2)G_1.K_s(t)$$
$$-90G_0^*G_1 = 0 \tag{a3}$$

and its solution is:

$$K_s(t) = a_6 + (-a_6 + K_s(0))\exp(-\frac{105G_0^* + 2}{\tau(105G_1^* + 2)}t)$$
$$a_6 = \frac{90G_0^*}{105G_0^* + 2}; G_0^* = \frac{K_0}{G_1} + \frac{K_0}{G2}; G_1^* = \frac{K_0}{G_1} \tag{a4}$$

Where $K_s(0)$ is the value of correction factor at *t*=0 which corresponds to the value *Ks* in the elastic case. The above equation has a nearly constant value for long times. For steady state solution (*t*→∞) and we have:

$$K_s(t)\Big|_{t=\infty} = \frac{90G_0^*}{105G_0^* + 2} \tag{a5}$$

For the case studies, it has the approximate value *Ks*=0.8537. So It seems that K_s =5/6 is an appropriate average value in this work.